Lower limit on the achievable temperature in resonator-based sideband cooling

M. Grajcar,[1,2] S. Ashhab,[1,3] J.R. Johansson,[1] and Franco Nori[1,4,5]

[1] *Frontier Research System, The Institute of Physical and Chemical Research (RIKEN), Wako-shi 351-0198, Japan*
[2] *Department of Experimental Physics, Comenius University, SK-84248 Bratislava, Slovakia.*
[3] *Physics Department, The University of Michigan, Ann Arbor, Michigan 48109-1040, USA*
[4] *Center for Theoretical Physics, Physics Department, Applied Physics Program, Center for the Study of Complex Systems, The University of Michigan, Ann Arbor, Michigan 48109-1040, USA*
[5] *CREST, Japan Science and Technology Agency (JST), Kawaguchi, Saitama 332-0012, Japan*

(Dated: February 11, 2008)

A resonator with eigenfrequency ω_r can be effectively used as a cooler for another linear oscillator with a much smaller frequency $\omega_m \ll \omega_r$. A huge cooling effect, which could be used to cool a mechanical oscillator below the energy of quantum fluctuations, has been predicted by several authors. However, here we show that there is a lower limit T^* on the achievable temperature, given by $T^* = T_m\omega_m/\omega_r$, that was not considered in previous work and can be higher than the quantum limit in realistic experimental realizations. We also point out that the decay rate of the resonator, which previous studies stress should be small, must be larger than the decay rate of the cooled oscillator for effective cooling.

PACS numbers: 85.85.+j, 45.80.+r

I. INTRODUCTION

Recently, a tremendous experimental effort has been devoted to the task of cooling mechanical oscillators below the energy of quantum fluctuations. In spite of many experimental improvements, the quantum limit has not been achieved.[1,2,3,4,5] Several papers that propose cooling mechanisms using electromagnetic (rf, microwave or light) resonators[6,7,8,9] or other cooling mechanisms[10,11,12,13,14,15] to fulfill this task have appeared recently. These papers predict an enormous cooling effect. However, they do not explicitly state that there is a lower limit on the achievable temperature, associated with the ratio between the frequencies of the coolant and cooled oscillators, that cannot be overcome and can play an important role for realistic experimental realizations. Moreover, some formulas that appear in the literature can give temperatures below this limit, which will be described in more detail below. This lower temperature limit can be important for the most feasible designs using rf or microwave resonators.

The electromagnetic resonators can be easily implemented on-chip beside a nano-mechanical oscillator and kept at low temperatures. Such structures, also known as MEMS and NEMS (micro and nanoelectromechanical systems), have already been realized[16,17,18], achieving high frequencies in the GHz range ($\omega_m \sim 10$ GHz) but with small quality factors $Q_m \sim 10 - 500$. Nevertheless, they can be used as sensitive elements for weak force-displacement detection[19,20] and they have been proposed as possible qubits.[21,22] For such systems, the frequency of the basic mode of the NEMS becomes comparable to the resonance frequency of the electromagnetic resonator ω_r. In this case, the temperature limit proportional to ω_m/ω_r which was negligible for optical-frequency coolers, can determine the lowest achievable temperature T^*. The aim of this work is to call the attention of experimentalists to this fundamental limit which could help them design more effective cooling systems.

II. SEMI-CLASSICAL APPROACH

For the sake of simplicity, we will consider a RLC tank circuit (the results can be applied to any electromagnetic resonator, such as a transmission-line resonator, cavity, Fabry-Perot resonator, etc.). A mechanical oscillator is coupled to the capacitor such that the capacitance depends parametrically on the displacement of the oscillator. Such a system was thoroughly analyzed in Ref. 23, and we only briefly introduce the equations of motion here. If the mechanical oscillator is a part of one of the capacitor electrodes, the capacitance $C(x) \approx C_0(1-x/d)$ depends on the displacement x of the oscillator from the equilibrium position, where $C_0 = \epsilon S/d_0$ is the capacitance at $x = 0$ and d is the renormalized distance between the electrodes $d = d_0/\kappa$. Here κ is the coupling constant between the mechanical oscillator and the RLC circuit, and it can be expressed as the ratio between the mechanical oscillator capacitance C_m, which depends on the oscillator displacement, and the total capacitance C_0 (we consider the case $C_m \ll C_0$), i.e. $\kappa = C_m/C_0$. If the RLC tank circuit is pumped by a microwave source $V_p = V_{p0}\cos\omega_p t$, the voltage between the capacitor's electrodes is $V_0 = \omega_r V_{p0}/\Gamma_r$, and the Coulomb energy of the capacitor depends on its capacitance which, in turn, depends on the oscillator displacement. Thus, the electromagnetic resonator and mechanical oscillator (i.e. cantilever) can be described by a system of differential

equations of two coupled damped linear oscillators

$$\frac{d^2Q}{dt^2} + \Gamma_r\frac{dQ}{dt} + \omega_r^2 Q\left(1-\frac{x(t)}{d}\right) = \frac{V_p(t)+V_f(t)}{L} \quad (1)$$

$$\frac{d^2x}{dt^2} + \Gamma_m\frac{dx}{dt} + \omega_m^2 x = \frac{F_f(t)}{M} + \frac{Q^2(t)}{2MC_0d} \quad (2)$$

where $\Gamma_{r,m}$ are damping rates, $\omega_{r,m}$ are angular frequencies, V_f is a fluctuating voltage across the capacitor, F_f is a fluctuating force acting on the mechanical oscillator with mass M, and $Q(t) = q_p(t) + q_f(t)$ is total charge charge on the capacitor. The Eq. (2) is nonlinear but can be linearized keeping in mind that we are interested to calculate charge fluctuations $q_f(t)$ which are much smaller than charge oscillations $q_p(t)$ driving by coherent microwave source. It is convinient to express $q_f(t)$ and $V_f(t)$ in terms of quadrature amplitudes

$$\begin{aligned} q_f(t) &= q_c(t)\cos\omega_p t + q_s(t)\sin\omega_p t \ , \\ V_f(t) &= V_c(t)\cos\omega_p t + V_s(t)\sin\omega_p t \ , \end{aligned}$$

and rewrite Eqs. (1),(2) in the dimensionless variables

$$\begin{aligned} \tilde{q}_{c,s} &\equiv q_{c,s}/\sqrt{C_0\hbar\omega_r} \ , \\ \tilde{x} &\equiv x/\sqrt{\hbar\omega_m/M\omega_m^2} \ , \\ \tau &\equiv \omega_m t \ , \\ \tilde{\omega}_{r,p} &\equiv \omega_{r,p}/\omega_m \ , \\ \tilde{\Gamma}_m &\equiv \Gamma_m/\omega_m \ , \\ \tilde{\Gamma}_r &\equiv \Gamma_r/2\omega_m \ , \\ \tilde{V}_{c,s} &\equiv \tilde{\omega}_r V_{c,s}\sqrt{C_0/\hbar\omega_r} \ , \\ \tilde{F}_f &\equiv F_f/\sqrt{M\omega_m^2\hbar\omega_m} \ , \\ \tilde{V}_0 &\equiv \tilde{\omega}_r V_0\sqrt{C_0/4M\omega_m\omega_r d^2}. \end{aligned}$$

Here T_r and T_m are the temperatures of the electromagnetic resonator and mechanical oscillator, respectively. Using the slowly-varying-amplitude approximation[23] and considering Langevin fluctuating forces caused by quantum noise,[24,25]

$$\begin{aligned} V_{c,s}(t) &= \sqrt{L\Gamma_r\frac{\hbar\omega_r}{2}\coth\left(\frac{\hbar\omega_r}{2k_BT_r}\right)}\xi_{c,s}(t) \ , \\ F_f(t) &= \sqrt{M\Gamma_m\hbar\omega_m\coth\left(\frac{\hbar\omega_m}{2k_BT_m}\right)}\xi_m(t) \ , \end{aligned}$$

Eqs. (1),(2) read

$$\frac{d\tilde{q}}{d\tau} = -\tilde{A}\,\tilde{q}(\tau) + \tilde{F}(\tau) \quad (3)$$

where

$$\tilde{A} = \begin{pmatrix} \tilde{\Gamma}_r & \tilde{\eta} & 0 & 0 \\ -\tilde{\eta} & \tilde{\Gamma}_r & 0 & -\tilde{V}_0 \\ -\tilde{V}_0 & 0 & \tilde{\Gamma}_m & 1 \\ 0 & 0 & -1 & 0 \end{pmatrix} , \quad (4)$$

$$\tilde{F}(\tau) = \begin{pmatrix} \sqrt{\tilde{\Gamma}_r\coth(\hbar\omega_r/2k_BT_r)}\xi_c(\tau) \\ \sqrt{\tilde{\Gamma}_r\coth(\hbar\omega_r/2k_BT_r)}\xi_s(\tau) \\ \sqrt{\tilde{\Gamma}_m\coth(\hbar\omega_m/2k_BT_m)}\xi_m(\tau) \\ 0 \end{pmatrix} , \quad (5)$$

$\tilde{q} \equiv (\tilde{q}_c, \tilde{q}_s, \tilde{v}, \tilde{x})$, $\tilde{v} \equiv d\tilde{x}/d\tau$ and $\tilde{\eta} = \tilde{\omega}_p - \tilde{\omega}_r$. Here T_r and T_m are the base temperatures of the resonator and mechanical oscillator, respectively. Thus, we have a system of coupled Langevin equations[24] which allow us to calculate the stationary covariance matrix defined as $\sigma \equiv \langle\tilde{q}\tilde{q}^T\rangle_s$ for $\tau\to\infty$. The diagonal terms of the covariance matrix determine the mean squared values of the vector components $\tilde{q}$. For example, $\sigma_{\tilde{v}\tilde{v}} \equiv \langle\tilde{v}^2\rangle_s$ is the normalized mean squared velocity of the mechanical oscillator. The covariance matrix can be determined from the system of linear equations

$$\tilde{A}\,\sigma + \sigma\tilde{A}^T = \tilde{B} \ ,$$

where $\tilde{B}$ is a correlation matrix defined as $\langle\tilde{F}_i(\tau)\tilde{F}_j(\tau')\rangle = \tilde{B}_{ij}\delta(\tau-\tau')$. If the fluctuating forces are uncorrelated, i.e. $\langle\xi_x(\tau)\xi_{x'}(\tau')\rangle = \delta_{x,x'}\delta(\tau-\tau')$ (here x, x' stand for c, s or m), $\tilde{B}$ takes the form of a diagonal matrix with elements

$$\tilde{B}_{ii} = \begin{pmatrix} \tilde{\Gamma}_r\coth(\hbar\omega_r/2k_BT_r) \\ \tilde{\Gamma}_r\coth(\hbar\omega_r/2k_BT_r) \\ \tilde{\Gamma}_m\coth(\hbar\omega_m/2k_BT_m) \\ 0 \end{pmatrix} . \quad (6)$$

The mean value of energy of the mechanical oscillator fluctuations is

$$\mathcal{E}_m = \sigma_{\tilde{v}\tilde{v}}\,\hbar\,\omega_m. \quad (7)$$

Now, one can easily calculate the effective temperature of the mechanical oscillator from the definition relation for T_m^*

$$\sigma_{\tilde{v}\tilde{v}} = \frac{1}{2}\coth\left(\frac{\hbar\omega_m}{2k_BT_m^*}\right) . \quad (8)$$

As we will see later, the most appropriate parameters for cooling purposes are $\tilde{\eta} = -1$, $2\tilde{\Gamma}_m\tilde{\Gamma}_r \ll \tilde{V}_0 \ll 1$. In this limit and for $\Gamma_r < \omega_m$, $\Gamma_m \ll \Gamma_r$ the $\sigma_{\tilde{v}\tilde{v}}$ can be expressed as

$$\sigma_{\tilde{v}\tilde{v}} = \frac{1}{2}\coth\left(\frac{\hbar\omega_r}{2k_BT_r}\right) + \frac{\tilde{\Gamma}_r\tilde{\Gamma}_m}{\tilde{V}_0^2}\coth\left(\frac{\hbar\omega_m}{2k_BT_m}\right) \quad (9)$$

Thus, the lowest temperature of the mechanical oscillator is limited by the first term if the second term is made negligibly small by sideband cooling. As a matter of fact this term simply shows that even in our semi-classical approach we cannot 'cool' the mechanical oscillator below the zero-point energy which is consistent with the Heisenberg uncertainty principle. Indeed, it follows from

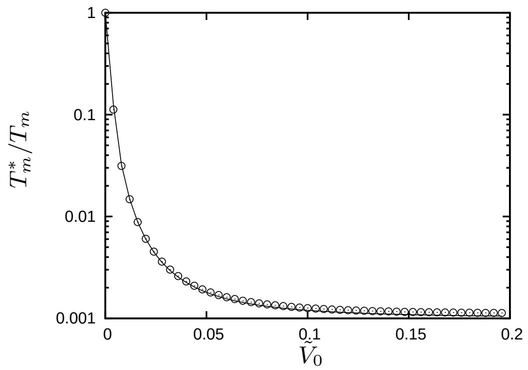

FIG. 1: The cooling factor T_m^*/T_m as a function of the normalized pumping amplitude $\tilde{V}_0$ of the noiseless microwave source for $\tilde{\omega}_r = 10^3$, $\tilde{\Gamma}_m = 10^{-5}$, $\tilde{\Gamma}_r = 10^{-1}$ and $k_B T_m = k_B T_r \gg \hbar\omega_{r,m}$ calculated numerically (circles) and from Eqs. (8),(9) (solid line).

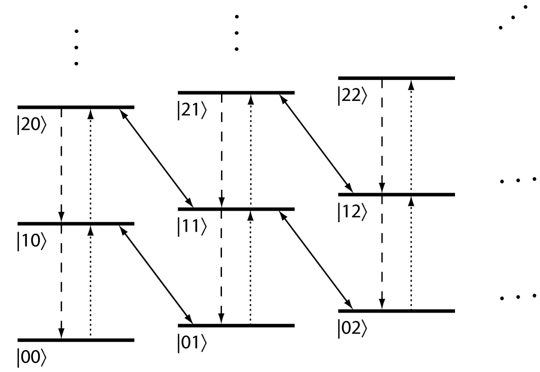

FIG. 2: Energy-level diagram of a high-frequency resonator and low-frequency mechanical oscillator with different possible transitions. The first and second quantum numbers represent the number of excitations in the resonator and mechanical oscillator, respectively. The vertical arrows represent the environment-induced decay in the resonator, and slanted arrows represent driving-induced transitions. Decay in the mechanical oscillator is assumed to be negligibly small.

Eqs.(7) and (8) that the energy saved in the mechanical oscillator is

$$\mathcal{E}_m = \frac{\hbar\omega_m}{2} \coth\left(\frac{\hbar\omega_r}{2k_B T_r}\right) \tag{10}$$

In this limit, the effective temperature T_m^* of the mechanical oscillator takes the simple form

$$T_m^* = \frac{\omega_m}{\omega_r} T_r \tag{11}$$

The cooling factor T_m^*/T_m as a function of the normalized pumping amplitude $\tilde{V}_0$ is shown in Fig. 1. Even though this result was derived within semi-classical physics, the same limit can be obtained using the quantum approach, as we shall show below.

Here we should emphasize that the temperature of the resonator T_r is usually much higher than the ambient temperature if the resonator is heavily pumped by the microwave source. This is caused by the phase noise of the microwave source, which is directly proportional to the output power. Microwave sources are characterized by the single sideband noise spectral density[27]

$$L(\Delta\omega) = 10 \log\left(\frac{S_V}{U_{mw}^2}\right) , \tag{12}$$

where U_{mw}^2 is the mean-square voltage of the microwave source and S_V is the spectral density of the voltage noise. The best commercially available microwave sources achieve $L(\Delta\omega) = -170$ dBc/Hz. The effective temperature T_r of the pumped resonator can be calculated as

$$T_r = T_{r0} + \frac{\omega_r}{\Gamma_r} \frac{U_{mw}^2}{2k_B Z_r} 10^{L(\Delta\omega)/10} \tag{13}$$

where T_{r0} is the temperature of the resonator without pumping and $Z_r = \sqrt{L/C}$ is the characteristic impedance of the resonator. Now, both terms in Eq. (9) depend on the pumping power. The first one increases with pumping power while the second one decreases. Since the highest cooling power is expected for[9] $\tilde{\Gamma}_r < 1$ the effective temperature of the mechanical oscillator is higher than

$$T_{m0} \approx \frac{U_{mw}^2}{2k_B Z_r} 10^{L(\Delta\omega)/10} . \tag{14}$$

Thus, for microwave resonators the first term in Eq. (9) becomes important, especially for the cooling of mechanical oscillators with high resonant frequencies approaching the GHz range. The minimal temperature T_{m0} is directly proportional to the pumping power in the limit $\tilde{V}_0 \ll 1$, which is the relevant limit in order to determine the lowest achievable temperature of the mechanical oscillator cooled by sideband cooling.

III. QUANTUM APPROACH

In order to achieve the quantum regime of the mechanical oscillator, the temperature should be lower than the energy of quantum fluctuations which, together with Eq. (11), imply the inequality

$$\frac{\omega_m T_r}{\omega_r} < T_m^* < \frac{\hbar\omega_m}{k_B} .$$

Thus the microwave resonator should be in the quantum regime as well, and the classical description is no longer valid. Therefore, we now turn to the analysis of this problem using the quantum description when the resonator's frequency is higher than its temperature and the resonator is in its ground state with high probability. The analysis is also valid if the resonator is substituted by a two-level system (qubit) as sugested in Ref. 10. In

this case the cooling limit can be derived in a transparent manner.

The Hamiltonian that we shall use in our analysis is given by

$$\hat{H} = \omega_r a_r^\dagger a_r + \omega_m a_m^\dagger a_m + \hat{H}_{\text{coupling}} + \hat{H}_{\text{drive}}, \quad (15)$$

where $a_r^\dagger$ and a_r ($a_m^\dagger$ and a_m) are, respectively, the creation and annihilation operators of the resonator (oscillator). The term $\hat{H}_{\text{coupling}}$ represents the oscillator-resonator coupling, and the term $\hat{H}_{\text{drive}}$ represents the driving force. We shall assume that the last two terms in the Hamiltonian are small: The smallness of $\hat{H}_{\text{coupling}}$ means that the energy eigenstates will, to a good approximation, be identified with well-defined excitation numbers in the oscillator and resonator, while the smallness of $\hat{H}_{\text{drive}}$ justifies a description of the system using time-independent energy levels. In the following we start by using thermodynamics arguments to derive an expression for the lower limit on the achievable temperature, and we later use a master-equation approach to treat the specific example discussed in Sec. II.

We first consider the situation depicted in Fig. 2. Each arrow describes a transition from a state $|i,j\rangle$ to another state $|i',j'\rangle$, where the meaning of the quantum numbers is explained in Fig. 2. We denote the rate at which such a transition occurs by $W_{|i,j\rangle\to|i',j'\rangle}$. In other words, the probability current of the transition is given by $P_{|i,j\rangle}W_{|i,j\rangle\to|i',j'\rangle}$, where $P_{|i,j\rangle}$ is the occupation probability of the state $|i,j\rangle$. In the steady state, we can write detailed-balance equations for the occupation probabilities of the different quantum states in the form

$$\begin{aligned} 0 = \frac{dP_{|i,j\rangle}}{dt} \; = \; & \left(W_{|i+1,j-1\rangle\to|i,j\rangle}P_{|i+1,j-1\rangle} - W_{|i,j\rangle\to|i+1,j-1\rangle}P_{|i,j\rangle}\right) + \left(W_{|i-1,j+1\rangle\to|i,j\rangle}P_{|i-1,j+1\rangle} - W_{|i,j\rangle\to|i-1,j+1\rangle}P_{|i,j\rangle}\right) \\ & + \left(W_{|i+1,j\rangle\to|i,j\rangle}P_{|i+1,j\rangle} - W_{|i,j\rangle\to|i+1,j\rangle}P_{|i,j\rangle}\right) + \left(W_{|i-1,j\rangle\to|i,j\rangle}P_{|i-1,j\rangle} - W_{|i,j\rangle\to|i-1,j\rangle}P_{|i,j\rangle}\right) \end{aligned} \quad (16)$$

Now we determine some relations among rates W. Let us start with situation when the driving force is switched off and the resonator is in contact with its surrounding environment, which is at temperature T_r. Assuming that the environment induces transitions between states that are different by one photon in the resonator, the rates must obey the thermal-equilibrium relation

$$\frac{W_{|i,j\rangle\to|i+1,j\rangle}}{W_{|i+1,j\rangle\to|i,j\rangle}} = \exp\left\{-\frac{\hbar\omega_r}{k_B T_r}\right\}. \quad (17)$$

Note that these transitions do not change the state of the mechanical oscillator, since without the driving force the oscillator and resonator are effectively decoupled ($\omega_m \ll \omega_r$). The oscillator is itself in contact with its environment at temperature T_m, but for optimal cooling we assume that the insulation is good enough that we can completely neglect environment-induced transitions, i.e. we have assumed that $W_{|i,j\rangle\to|i,j\pm1\rangle} \to 0$ in Fig. 2 and Eq. (16). We now assume that the driving force couples states of the form $|i,j\rangle$ and $|i+1,j-1\rangle$ but does not drive any other transitions. Since the driving force is a classical one, the transitions it induces must have equal rates in both directions, i.e.

$$W_{|i,j\rangle\to|i+1,j-1\rangle} = W_{|i+1,j-1\rangle\to|i,j\rangle}. \quad (18)$$

The reason why there is no Boltzmann factor in Eq. (18) is that these transitions are mainly induced by the classical driving force, and any contributions to their rates from the thermal environment are negligible.

Using Eqs. (17) and (18), it is not difficult to verify that the pairs of terms in Eq. (16) all vanish when

$$P_{|i,j\rangle} = \frac{1}{Z}\exp\left\{-\frac{(i+j)\hbar\omega_r}{k_B T_r}\right\}, \quad (19)$$

where Z is the partition function. This steady-state probability distribution $P_{|i,j\rangle}$ can now be rewritten as

$$\begin{aligned} P_{|i,j\rangle} &= \frac{1}{Z_r}\exp\left\{-\frac{i\hbar\omega_r}{k_B T_r}\right\} \times \frac{1}{Z_m}\exp\left\{-\frac{j\hbar\omega_r}{k_B T_r}\right\} \\ &= \frac{1}{Z_r}\exp\left\{-\frac{i\hbar\omega_r}{k_B T_r}\right\} \times \frac{1}{Z_m}\exp\left\{-\frac{j\hbar\omega_m}{k_B T_m^*}\right\}, \end{aligned} \quad (20)$$

with

$$\frac{T_m^*}{T_r} = \frac{\omega_m}{\omega_r}. \quad (21)$$

Here Z_r and Z_m is partition function of resonator and mechanical oscillator, respectively. We therefore find that if the above picture about the allowed transitions and the relations governing their rates are valid, we can reach the final temperature T_m^* given by Eq. (21).

The above derivation suggests an intuitive picture for the cooling mechanism. The purpose of the driving force is to facilitate the transfer of excitations between the resonator and oscillator. Before the driving starts, the low-frequency oscillator has many more excitations than the high-frequency resonator. Once the driving starts, the excitation imbalance causes excitations to start flowing from the oscillator to the resonator. As the number of excitations in the resonator goes above the thermal-equilibrium value, excitations start to dissipate from the

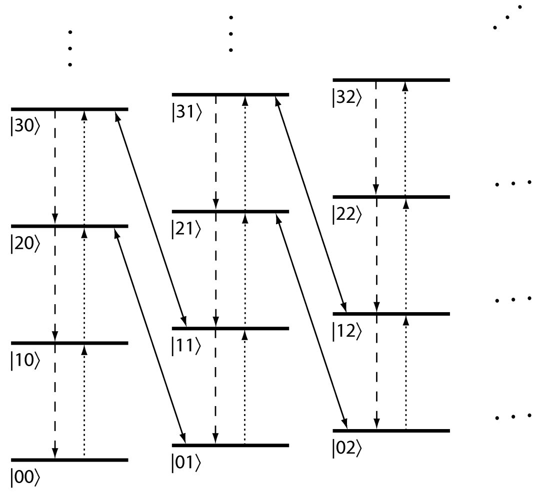

FIG. 3: Same as in Fig. 2, but with the driving force inducing a different type of transitions. The driven transitions in this case remove one excitation from the oscillator state and add two excitations to the resonator state, or vice versa.

resonator to the environment. A steady state is eventually reached with the resonator in thermal equilibrium with the environment and both the resonator and the oscillator having the same average number of excitations (in fact, the resonator and the oscillator will have the same excitation-number probability distribution). This picture of the cooling mechanism reveals another point that is generally not noted in the literature. Although Γ_r is desired to be smaller than ω_m in order to avoid heating effects, it should not be too small, because it provides the mechanism by which excitations are dissipated from the resonator into the environment. In particular, it must be larger than Γ_m, such that the dissipation of excitations is faster than the heating of the oscillator by its environment.

We now consider what would happen if one were able to drive transitions as shown in Fig. 3. With optimal parameters for cooling, one would obtain the minimum temperature

$$\frac{T_m^*}{T_r} = \frac{\omega_m}{2\omega_r}. \tag{22}$$

Note that this situation would require driving the system at a frequency $2\omega_r - \omega_m$. The argument can be generalized to obtain any value n in the denominator of Eq. (22), or more explicitly

$$\frac{T_m^*}{T_r} = \frac{\omega_m}{n\,\omega_r}. \tag{23}$$

The question is whether such transitions can be realistically driven in a given system with a specific form of resonator-oscillator coupling and a given type of driving force.

In order to determine the feasibility of realizing conditions where Eq. (23) with $n > 1$ is the relevant lower limit on the achievable temperature, we now turn from the above general arguments to the specific situation considered in Sec. II. Equations (1),(2) result from a Hamiltonian of the form

$$\begin{aligned} \hat{H} &= \omega_r a_r^\dagger a_r + \omega_m a_m^\dagger a_m + g\left(a_r + a_r^\dagger\right)^2\left(a_m + a_m^\dagger\right) \\ &+ A\cos(\omega_p t + \theta)\left(a_r + a_r^\dagger\right), \end{aligned} \tag{24}$$

where g is the oscillator-resonator coupling strength, and A is the amplitude of the driving force. Starting with a simplified version of the above Hamiltonian that does not contain the last two terms, we have an energy-level diagram similar to the one shown in Fig. 2 (without the induced-transition arrows). The resonator-oscillator coupling term mixes the different quantum states together in the eigenstates of the Hamiltonian. This mixing allows the driving term, which would normally affect only the resonator, to drive transitions that remove excitations from the oscillator and add excitations to the resonator, or vice versa. Therefore, in order to determine the transitions that can be driven by the external force, we need to evaluate matrix elements of the form $\langle\psi_{i,j}|(a_r + a_r^\dagger)|\psi_{k,l}\rangle$, where we now use the eigenstates of the Hamiltonian (i.e. slightly modified from the case of two uncoupled oscillators). To first order in perturbation theory,

$$\begin{aligned} |\psi_{i,j}\rangle &\approx |i,j\rangle + \frac{(2i+1)g}{\omega_m}\left(\sqrt{j}|i,j-1\rangle - \sqrt{j+1}|i,j+1\rangle\right) \\ &+ \frac{g}{2\omega_r - \omega_m}\left(\sqrt{i(i-1)(j+1)}|i-2,j+1\rangle - \sqrt{(i+1)(i+2)j}|i+2,j-1\rangle\right). \end{aligned} \tag{25}$$

Using the above approximation, we find that

$$\langle\psi_{i,j}|a_r + a_r^\dagger|\psi_{i+1,j-1}\rangle \approx -\frac{2g\sqrt{(i+1)j}}{\omega_m}. \tag{26}$$

It is straightforward to see from Eq. (24) that

$$\langle\psi_{i,j}|a_r + a_r^\dagger|\psi_{i+2,j-1}\rangle = 0\ .$$

Using numerical calculations we find that

$$\langle\psi_{i,j}|a_r+a_r^\dagger|\psi_{i+3,j-1}\rangle \approx -\frac{12g^3\sqrt{(i+1)(i+2)(i+3)j}}{(2\omega_r-\omega_m)^3}. \quad (27)$$

The above results imply that the driving term can be used to drive transitions of the form $|i,j\rangle \leftrightarrow |i+1,j-1\rangle$, which can be used to remove excitations from the oscillator and add them to the resonator. These transitions correspond to the picture shown in Fig. 2, and their resonance frequency is given by $\omega_p=\omega_r-\omega_m$. The steady-state effective temperature for the oscillator is given by Eq. (21) when driving these transitions, assuming that heating effects are avoided. By driving the system at the frequency $\omega_p=3\omega_r-\omega_m$, one could in principle drive the transitions $|i,j\rangle \leftrightarrow |i+3,j-1\rangle$ and reach a lower minimum temperature. However, the fact that the corresponding matrix element is proportional to the third power of the small coupling strength g suggests that this matrix element will be extremely small for any realistic parameters, hindering the possibility of utilizing this cooling mechanism.

We now turn to the heating effects that have been neglected above. We note that the driving term in Eq. (24) can also drive transitions of the form $|i,j\rangle \leftrightarrow |i+1,j+1\rangle$, and the relevant matrix element is given by

$$\langle\psi_{i,j}|a_r+a_r^\dagger|\psi_{i+1,j+1}\rangle \approx \frac{2g\sqrt{(i+1)(j+1)}}{\omega_m}. \quad (28)$$

These undesired transitions are induced if either the driving amplitude A or the resonator's damping rate Γ_r is comparable to or larger than ω_m. If either one or both of the above conditions are satisfied, the driving force must be considered within the resonance region of the above transition. As a result, additional excitation would be steadily pumped into the system, resulting in a higher temperature than what would be obtained from the simple picture of transition rates that we have presented above. The ideal parameters for cooling are therefore given by $\omega_p=\omega_r-\omega_m$, $A \ll (\omega_r-\omega_p)$ and $\Gamma_r \ll (\omega_r-\omega_p)$; naturally Γ_m is desired to be much smaller than both Γ_r and A^2/Γ_r, such that the oscillator heating from its contact with the environment is slower than the cooling it experiences as a result of the driving. Using a numerical simulation, we shall see shortly that the above heating effects can be made negligible with the proper choice of parameters. We should also mention here that in this section we have not considered the noise in the driving force, i.e. we have assumed a perfect microwave source. Such noise would directly heat the resonator, resulting in a higher base temperature, as discussed in Sec. II.

In order to give a concrete example that illustrates the cooling dynamics, we now turn to a master-equation approach. The density matrix ρ of the system evolves in time according to the master equation

$$\begin{aligned}\frac{d\rho}{dt} &= -\frac{i}{\hbar}\left[\hat{H},\rho\right] + \left(1+\bar{N}_r\right)\Gamma_r\left(a_r\rho a_r^\dagger - \frac{1}{2}a_r^\dagger a_r\rho - \frac{1}{2}\rho a_r^\dagger a_r\right) + \bar{N}_r\Gamma_r\left(a_r^\dagger\rho a_r - \frac{1}{2}a_r a_r^\dagger\rho - \frac{1}{2}\rho a_r a_r^\dagger\right)\\ &\quad + \left(1+\bar{N}_m\right)\Gamma_m\left(a_m\rho a_m^\dagger - \frac{1}{2}a_m^\dagger a_m\rho - \frac{1}{2}\rho a_m^\dagger a_m\right) + \bar{N}_m\Gamma_m\left(a_m^\dagger\rho a_m - \frac{1}{2}a_m a_m^\dagger\rho - \frac{1}{2}\rho a_m a_m^\dagger\right), \quad (29)\end{aligned}$$

where

$$\bar{N}_r = \frac{1}{e^{\hbar\omega_r/k_BT}-1} \quad (30)$$

and similarly for $\bar{N}_m$. The coefficients Γ_r and Γ_m are decay rates for the resonator and oscillator, respectively.

An example illustrating the dynamics of cooling the mechanical oscillator by the microwave resonator is shown in Fig. 4. The results were obtained by numerically solving Eq. (29) using the Hamiltonian in Eq. (24). The effective temperatures of the oscillator and resonator are obtained by calculating their respective entropies from their reduced density matrices ($S=-\mathrm{Trace}\{\rho\log\rho\}$) and fitting these values to the temperature-entropy relation for a harmonic oscillator. The initial heating of the resonator is a result of the transfer of excitations from the oscillator to the resonator. For large t, the system reaches a steady state where the ratio between the effective temperatures of the oscillator and the resonator is approximately equal to ω_m/ω_r.

IV. CONCLUSIONS

We have shown that both the classical and the quantum treatment give the same final result: the cooling factor T_m^*/T_r is limited by the ratio ω_m/ω_r. This lower limit for the cooling becomes crucial for rf and microwave resonators pumped by a real (noisy) microwave source since their effective temperature T_r is usually much larger than the ambient temperature. We should also emphasize that our results apply, with minor modifications, to other types of coolers, e.g. a cooper-pair box.

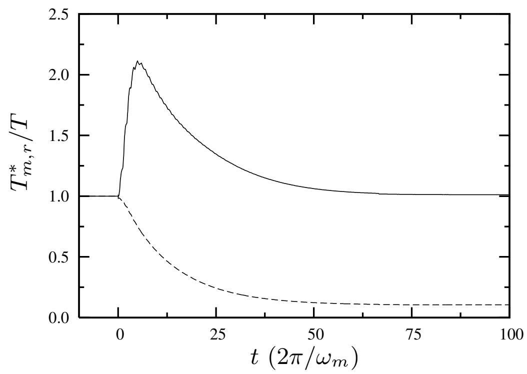

FIG. 4: Effective temperatures for the resonator (solid line) and the oscillator (dashed line), relative to the ambient temperature, as a function of time for the parameters $\omega_m/\omega_r = 0.1$, $g/\omega_r = 0.005$, $k_B T_{m,r}/\hbar\omega_r = 0.5$, $\Gamma_r/(\omega_r/2\pi) = 0.05$, and $\Gamma_m = 0$. The driving field, with amplitude $A/\omega_r = 0.05$ and frequency $\omega_p = \omega_r - \omega_m$, is turned on at $t = 0$.

Acknowledgments

This work was supported in part by the National Security Agency (NSA), the Laboratory for Physical Sciences (LPS), the Army Research Office (ARO), the National Science Foundation (NSF) grant No. EIA-0130383 and the Japan Society for the Promotion of Science Core-To-Core (JSPS CTC) program. M.G. was partially supported by Grants VEGA 1/0096/08, APVT-51-016604 and Center of Excellence of the Slovak Academy of Sciences (CENG).

[1] M. D. LaHaye, O. Buu, B. Camarota, and K. C. Schwab, Science **304**, 74 (2004).
[2] K. C. Schwab and M. L. Roukes, Physics Today **58**, 36 (2005).
[3] S. Gigan, H. R. Böhm, M. Paternostro, F. Blaser, G. Langer, J. B. Hertzberg, K. C. Schwab, D. Bäuerle, M. Aspelmeyer, and A. Zeilinger, Nature **444**, 67 (2006).
[4] A. Schliesser, P. Del'Haye, N. Nooshi, K. J. Vahala, and T. J. Kippenberg, Phys. Rev. Lett. **97**, 243905 (2006).
[5] K. R. Brown, J. Britton, R. J. Epstein, J. Chiaverini, D. Leibfried, and D. J. Wineland, arXiv.org:0705.1197v1.
[6] I. Wilson-Rae, P. Zoller, and A. Imamoglu, Phys. Rev. Lett. **92**, 075507 (2004).
[7] F. Marquardt, J. P. Chen, A. A. Clerk, and S. M. Girvin, Phys. Rev. Lett. **99**, 093902 (2007).
[8] I. Wilson-Rae, N. Nooshi, W. Zwerger, and T. J. Kippenberg, Phys. Rev. Lett. **99**, 093901 (2007).
[9] F. Xue, Y. D. Wang, Y. X. Liu, and F. Nori, Phys. Rev. B **76**, 205302 (2007).
[10] I. Martin, A. Shnirman, L. Tian, and P. Zoller, Phys. Rev. B **69**, 125339 (2004).
[11] W. K. Hensinger, D. W. Utami, H.-S. Goan, K. Schwab, C. Monroe, and G. J. Milburn, Phys. Rev. A **72**, 041405(R) (2005).
[12] M. Grajcar, S. H. W. van der Ploeg, A. Izmalkov, E. Il'ichev, H. G. Meyer, A. Fedorov, A. Shnirman, and G. Schön, arXiv.org:0708.0665.
[13] J. Q. You, Y. X. Liu, and F. Nori, Phys. Rev. Lett **100**, 047001 (2008).
[14] It is worth mentioning here that similar sideband cooling mechanisms have appeared in different contexts over the years. See, e.g., M. I. Dykman, Sov. Phys. Solid State **20**, 1306 (1978).
[15] H. Quan, Y. X. Liu, C. P. Sun, and F. Nori, Phys. Rev. E **76**, 031105 (2007).
[16] X. Huang, C. A. Zorman, M. Mehregany, and M. L. Roukes, Nature **421**, 496 (2003).
[17] V. Sazanova, Y. Yaish, T. A. A. H. Üstünel, D. Roundy, and P. L. McEuen, Nature **431**, 284 (2004).
[18] H. B. Peng, C. W. Chang, S. Aloni, T. D. Yuzvinsky, and A. Zettl, Phys. Rev. Lett. **97**, 087203 (2006).
[19] L. F. Wei, Y. X. Liu, C. P. Sun, and F. Nori, Phys. Rev. Lett. **97**, 237201 (2006).
[20] G. J. Milburn, C. A. Holmes, L. M. Kettle, and H. S. Goan, arXiv.org:cond-mat/0702512.
[21] S. Savel'ev, X. Hu, and F. Nori, New J. Phys. **8**, 105 (2006).
[22] J. Q. You and F. Nori, Physics Today **58**, 42 (2005).
[23] V. Braginsky and F. Khalili, *Quantum Measurement* (Cambridge University Press, Cambridge, 1992).
[24] C. Gardiner, *Handbook of Stochastic Methods* (Springer, Berlin, 1995).
[25] C. W. Gardiner and P. Zoller, *Quantum Noise* (Springer-Verlag, Berlin, 2000).
[26] M. I. Dykman, Sov. Phys. Solid State **20**, 1306 (1978).
[27] T. H. Lee and A. Hajimiri, IEEE J. Solid-State Circuits **35**, 326 (2000).